33rd Annual International Conference of the IEEE EMBS
Boston, Massachusetts USA, August 30 - September 3, 2011

A Novel Method of Detection and Classification of Motor Nerve Late-wave Activity

D. Iyer, PhD, L. Zheng, PhD, M. L.Williams, PhD, B. H. Tracey, PhD, S. N. Gozani, MD, PhD, *Members, IEEE*

Abstract— **In motor nerve conduction studies, important diagnostic information is provided by the late-wave responses, comprised of F-waves, A-waves, and repeaters. Late-waves in addition to contamination from power line interference and baseline disturbance, are of low amplitude and random in nature. This makes computer-based analysis of late-wave activity very challenging, especially the computer-based F-wave onset latency assignment. Currently available algorithms assign latency independently on a trace-by-trace basis without considering the information present in an entire ensemble of traces. A novel algorithm that takes into account the ensemble information for segmenting and classifying regions of late-wave data is described in this paper, which in turn can be used to improve the performance of computer-based F-wave onset latency assignment.**

I. INTRODUCTION

Nerve conduction studies (NCS) serve as an important tool in assessing the integrity of the peripheral nerves [1, 2, 7]. In motor NCS, an electrical stimulus is used to locally depolarize a short segment of the motor nerve. If the depolarization is of sufficient magnitude, a compound action potential is induced in a number of axons within the nerve, which propagates both distally and proximally from the point of stimulation.

The distally-propagating (orthodromic) compound action potential reaches the muscle and activates neurotransmitter release at the neuromuscular junction, causing muscle contraction. The resulting electrical activity measured at the muscle is referred to as compound motor action potential (CMAP). Normally, the latency and morphology of CMAP remain stable from one stimulus to the next.

The proximally-propagating (antidromic) compound action potential reaches the spinal cord, causing a small and random fraction of the motor neurons to "backfire", resulting in a new, distally-traveling compound action potential that travels back to the muscle. The responses of the muscle due to this back-propagating action potential are called F-waves [4]. Unlike CMAP, the latency and morphology of F-waves typically vary significantly from one stimulus to the next. Because only a small fraction of the neurons participate, F-waves are much smaller in amplitude than CMAP.

F-waves are the most common type of "late waves" (so-named as they arrive after the CMAP). In some subjects, a small set of neurons (called "Repeaters") have a high probability of backfiring and produce features with similar morphology across multiple recordings. In other subjects, axonal branching may exist. This branching produces waveform components that repeat with constant latency across multiple recordings. These constant feature components usually occur before the F-waves and are often referred to as A-waves. Repeaters and A-waves can be important indicators of neuromuscular pathology along the full length of the nerve, and are grouped together in this paper as both lead to repeating waveform features.

In traditional NCS, the detection and classification of late-wave activity is done manually or with the aid of simple computer algorithms [3, 6]. A physician will assign or confirm F-wave latencies and note the existence of any A-waves or Repeaters. In recent years, technological advances have led to the introduction and large-scale adoption of point-of-service NCS testing [1], which in turn need algorithms that can automatically and accurately analyze late-wave data.

Late-wave analysis is complicated by the random nature and low amplitude of late waves. Currently available algorithms [4] assign latency independently on a trace-by-trace basis without considering the entire ensemble of traces. As a consequence, such algorithms are vulnerable to fasciculation and other artifacts. In addition, they are counter intuitive to the way human experts would manually analyze the data, who typically examine the entire ensemble of traces to identify regions of consistent activity before assigning latency on each trace.

We addressed this issue in our previous work [5], where we developed a segmentation approach to analyze the entire ensemble of traces and identify portions of the data with consistent late-wave activity, followed by clustering-based approach to classify segments as F-wave or A-wave/Repeater.

However, different sets of features were being used to calculate F-waves and A-waves separately, which was computationally very intensive and needed several parameters. In addition, the clustering approach was very demanding, both in terms of algorithm complexity and computational resources. In this paper, we present a recently developed technique, which is much simpler in terms of

D. Iyer (e-mail: darshan_iyer @neurometrix.com), M.L. Williams, S.N. Gozani are with NEUROMetrix, Inc., 62 Fourth St, Waltham MA 02451.

L. Zheng was previously with NEUROMetrix, Inc., and is now with Draeger Medical Systems, Inc., Andover, MA- 01810.

B.H. Tracey was previously with NEUROMetrix, Inc., and is now with Tufts University, Medford, MA 02155.

number of parameters and algorithm complexity, and is much faster and gives comparable performance. The algorithm follows a systematic and streamlined approach. In addition, the clustering method used to classify segments depends on fewer features and is much simpler.

II. METHODS

A. Data

The NCS data used in this study were acquired with ADVANCE^{TM} developed by NeuroMetrix, Inc (Waltham MA 02451 USA). Integrated pre-configured electrode arrays with stimulator, detector, and reference electrodes are used. A constant current stimulator is used. Data processing is done on the device using algorithms that analyze waveforms and adjust stimulus current.

During testing, the stimulator current and amplitude are adjusted until the CMAP response reaches a maximal level. This indicates that the stimulus is sufficient to excite all motor fibers in the nerve. Once the maximal level is determined, a series of stimuli are applied. A recording is made which includes both the CMAP and late-wave time periods. Late-wave data are digitally downsampled to a 5 kHz sampling rate. The late-wave signals are collected to form an ensemble of late-wave traces (see Figure. 1 for example). The number of traces collected depends on the nerve being analyzed (10 for upper extremity nerve and 16-32 for lower extremity nerve).

A set of 406 late-wave datasets was collected, consisting of approximately 100 tests each from median, ulnar, peroneal, and tibial nerves.

B. Preprocessing steps

Late-waves may be distorted by the presence of power line contamination and/or baseline disturbance resulting from residual CMAP activity. Preprocessing is done to remove these sources of contamination. Figure 1 shows an example of contaminated late-wave data along with the results of preprocessing.

Due to overlapping spectra of power line interference (PLI) and late waves, any linear bandstop filter with non-zero bandwidth will affect the morphology of late waves. As an alternative, the phase and amplitude of a sine wave at the PLI fundamental frequency are estimated from the signal-free region of the trace to obtain least-squares fit, which is then subtracted from the entire trace.

Baseline disturbances (BD) are the most significant source of contamination, especially for upper extremity nerves. BD is due to residual CMAP activity, which has significantly higher amplitude than late waves and have relatively consistent morphology as described earlier. As a result, the BD tends to be stable across traces which can be exploited in estimating the BD shape. BD removal is important as otherwise the algorithm might incorrectly identify the consistent BD features as A-wave/repeater activity.

BD is estimated using a weighted least-squares fit to a piecewise polynomial model, where in the fit is weighted by the $1/\sigma^2$ (σ^2 is variance of same time samples across all the traces) to avoid fitting the BD model to regions where F-waves may be present. Relatively low order polynomials (5^{rd} – 6^{th} order) are used to prevent the polynomial fit from introducing artificial late-wave features. The break-point between piecewise polynomial sections is found by detecting an onset of overall F-wave activity ascertained from σ^2.

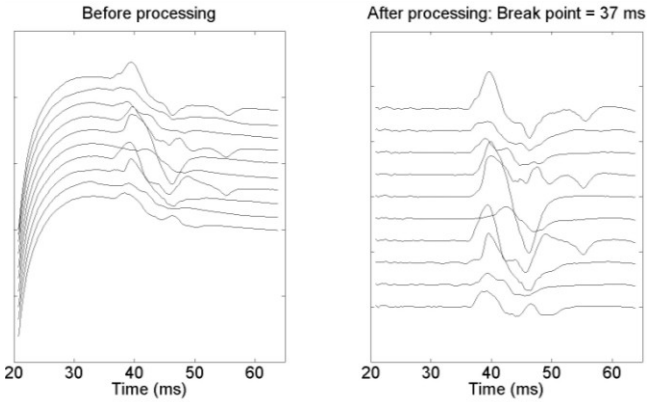

Fig. 1 An ensemble of late-wave traces with BD. The ensemble is shown before (left panel) and after preprocessing (right panel).

C. Segmentation

As depicted in Figure. 2, preprocessed data are fed into the segmentation algorithm which detects and classifies late wave data into A-waves and F-waves. The entire algorithm is inspired by the way a human expert analyzes the late-wave data. The expert begins with finding groups of "consistent" regions, followed by identifying regions with similar or variable activity. The regions with high similarity are labeled as A-waves and regions with little or no similarity are labeled as F-waves. Each test consists of at the most only one F-wave segment and zero or more A-wave segments.

In the first step, we calculate an activity measure to identify regions of consistent activity. The activity measure A is calculated for each time n instant by computing the arithmetic mean of the absolute value of data across traces (total L traces) at that instant as

$$A(n) = \frac{1}{L-1}\sum_{i=1}^{L} X_{i,n}\Big| \qquad (1),$$

followed by smoothing with a moving-average (boxcar) filter; i is the trace index. Samples that are consistent across traces will have high activity measure values. The activity measure is then adjusted for noise floor by subtracting a noise estimate. A threshold (equal to minimum of a preset threshold and a percentage of maximum activity value) is applied to the adjusted activity measure to find consistent and distinct regions.

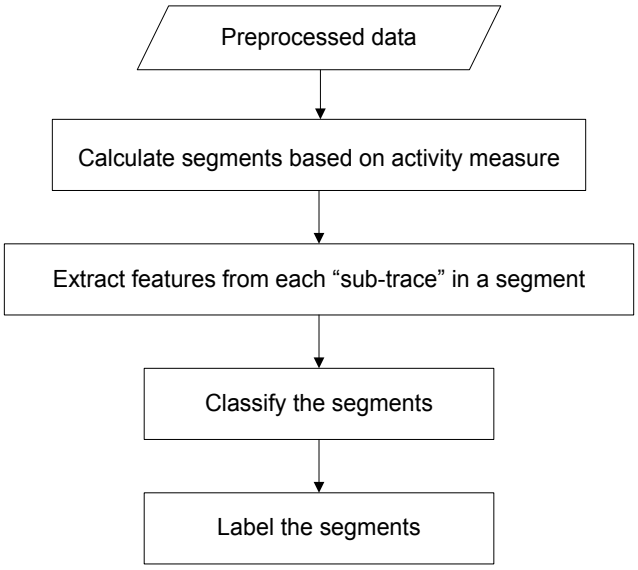

Fig. 2 Segmentation process.

The activity measure is converted into a Boolean sequence of ones and zeros by comparing the measure against the above threshold; samples that exceed the threshold are the qualifying samples. Morphological operation of dilation is done to fill any narrow gaps between groups of qualifying samples, followed by an erosion operation to discard very narrow groups. All contiguous groups of qualifying activity samples are identified, where each group constitutes a segment. The beginning and the end of each segment is adjusted to the local minima of the activity measure to ensure that the entire duration of segment is captured and each segment is complete in itself. Finally, only the segments that meet minimum duration requirement and have sufficient persistence are retained, where persistence is defined as ratio of number of traces with global peak-to-peak amplitude above certain threshold to the total number of traces.

Once segments have been identified, the portions of the traces within each segment ("sub-traces") are grouped into clusters based on their morphological similarity. This similarity is quantified using a set of features calculated from each sub-trace. The features include global peak-to-peak amplitude, root-mean-squared value (*RMS*), wave period (*Tp*), center of mass (*Cm*), and best peak. Global peak-to-peak is the difference between maximum and minimum value within each sub-trace; *RMS* for each sub-trace is calculated by squaring all the values, followed by finding the arithmetic mean of the squared values, and finally finding the square root of the mean value; *Tp* is calculated as

$$Tp = \frac{1}{2\pi}\frac{RMS_x}{RMS_y} \qquad (2),$$

where, x is a sub-trace, and y is a derivative of x approximated as the first-order difference. *Cm* is calculated as

$$Cm = \frac{\sum_i |x_i . i|}{\sum_i |x_i|} \qquad (3),$$

where i is the sample index. Best peak is calculated by finding the indices corresponding to global maximum and global minimum within each sub-trace, followed by finding the index with a larger absolute value.

Sub-traces are clustered using the above set of features and based on persistence, cluster energy (calculated as ratio of sum of squared values of the sub-traces within the cluster to the sum of squared values of all the sub-traces within the segment), and global peak-to-peak amplitude of the sub-traces within each segment. A segment is classified as "similar-high", "similar-low", "similar-noisy", and "not similar". A segment - is classified as "similar-high" if sub-traces are highly similar, have global peak-to-peak amplitude above a certain threshold, and have high cluster energy; as "similar-noisy" if sub-traces have high similarity and have global peak-to-peak amplitude above certain threshold, but lower cluster energy; as "similar-low" if sub-traces are highly similar, but global peak-to-peak amplitude is below certain threshold. The remaining segments are labeled as "not similar".

In the final stage of segmentation, segments classified as "similar-high" are labeled as A-segments, "similar-noisy" are labeled as A+F-segments, "not similar" are as F-segments, and "similar-low" are dropped (as these look like A-waves but are not due to low global peak-to-peak amplitude). Of all the A+F and F segments, the one with the largest normalized energy (energy normalized by segment length) is the final F-segment. The rest of the F-segments are discarded, and A+F segments are relabeled as A-segments. As mentioned earlier, a dataset can have at the most only one F-segment and zero or more A-segments. Figure 3 depicts an example of outputs at different stages in segmentation.

D. Performance Evaluation

For F-wave analysis, the clinical parameter of greatest interest is the F-wave latency, defined as the onset time for late-wave activity. Once the late-wave data are segmented and classified into different regions, F-wave segments are fed into the F-wave latency assignment algorithm to limit the latency search to segments.

For evaluating the performance of segmentation, F-wave latencies with and without the segmentation step were computed for each test and both were compared with the assignments by a board-certified neurologist. The comparison was done using the mean F-wave latency calculated as the arithmetic mean of the individual F-wave latencies. Mean (μ) and standard deviation (σ) depicting the expert-algorithm bias and Pearson correlation coefficient (ρ) values are reported for the two comparisons.

III. RESULTS AND DISCUSSION

Compared to our previous work [5], the algorithm presented here resulted in reduction in parameter space by 70%, increase in speed by 70 %, and reduction in code space by 80%.

Figure 4 shows an example depicting the output of latency assignment algorithm, with and without segments. Without segments, the latency assignments are highly susceptible to fasciculations and other artifacts, resulting in several outlier latencies. With segmentation, the estimated latencies are much more intuitive and follow a trend which is consistent with how a human expert would analyze the data. A description of the latency algorithm is outside the scope of this paper. However, as depicted in Table 1, latency results were significantly better ($p<0.05$) after segmentation by comparison to manual assignments by a neurologist.

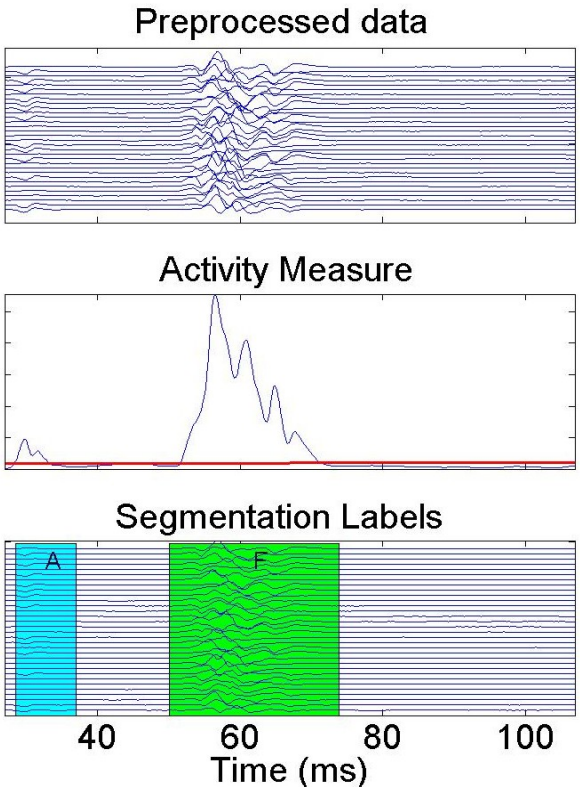

Fig. 3 Example of outputs at different stages in segmentation. Top: ensemble of preprocessed data; middle: activity measure; bottom: output labeled segments. The red line in the middle panel indicates the threshold used to find "consistent" activity regions.

IV. CONCLUSION

A new and improved approach to segmenting and classifying regions of late-wave activity has been described in this paper. The algorithm finds portions of consistent activity, followed by clustering and classification of the regions into A-waves and F-waves. The performance of F-wave latency assignment can be drastically improved by providing as input only the data corresponding to F-wave segments, thereby limiting the latency search to F-wave segments. The segmentation approach presented here is general enough to be applied to any data consisting of ensemble of traces with consistent activity and similar and/or dissimilar features.

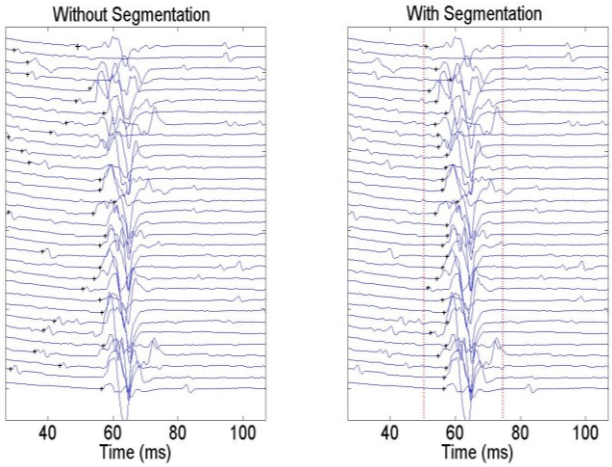

Fig 4. Effect of segmentation on latency assignments. The left panel shows the latencies ('+') without any segments; the right panel depicts enhanced performance when latencies were constrained to be within segments.

	Expert Vs No Segment	Expert Vs Segmented
Lower Extremity		
$\mu\pm\sigma$	1.71±5.16	0.48±2.27
ρ	0.73 [0.65 0.80]	0.94 [0.92 0.96]
Upper Extremity		
$\mu\pm\sigma$	1.68±1.29	1.37±0.72
ρ	0.92 [0.89 0.94]	0.98 [0.97 0.98]

Table 1. Bias ($\mu\pm\sigma$) and Pearson correlation coefficient (ρ) values along with confidence interval comparing expert assignments with algorithm assignments without and with segmentation. The results with segmentation were significantly better at 95% confidence level.

REFERENCES

[1] Kimura J. *Electrodiagnosis in Diseases of Nerve and Muscle: Principles and Practice*, 2nd ed. Philadelphia PA: Davis 1989.

[2] S.N. Gozani, M.A. Fisher, X. Kong, J.T. Megerian, and S.B. Rutkove, "Electrodiagnostic automation: principles and practice," Phy. Med. Rehabil. N. Am., 16: 1015-1032, 2005.

[3] Fisher MA. "Comparison of automated and manual F-wave latency measurements", Clin Neurophysiol.; 116(2):264-269, Feb 2005.

[4] Kong X, Gozani SN. "F-Wave" in Wiley Encyclopedia of Biomedical Engineering (Akay M Editor), 3: 1714-1725, John Wiley & Sons, 2006.

[5] Krishnamachari S., Tracey B. H., Iyer D., Detection and Classification of Motor Nerve Late-Wave Activity, Conf Proc IEEE Eng Med Biol Soc.; 1441-1444, 2007.

[6] Tracey BH, Iyer D, Lesser EA, Potts FJ, Gozani, SN. Comparison of expert and algorithm agreement in measurement of nerve conduction study parameters. Technical Note. Biomedical Signal Processing and Control. 5(2): 158-163, April 2010.

[7] Kong X, Lesser EA, Gozani SN. "Nerve conduction studies: clinical challenges and engineering solutions", IEEE Eng Med Biol Mag.; 29(2): 26-36, March-April 2010.